

Chapter 2

Deeply Inelastic Scattering

Deep—inelastic scattering experiments provide one of the cleanest possibilities to probe the space—like short distance structure of hadrons through the reactions

$$l^{\pm} N \rightarrow l^{\pm} + X \quad (2.1)$$

$$\nu_l(\bar{\nu}_l) N \rightarrow l^{\mp} + X \quad (2.2)$$

$$l^{\mp} N \rightarrow \nu_l(\bar{\nu}_l) + X, \quad (2.3)$$

with $l = e, \mu$, $\nu_l = \nu_{e,\mu,\tau}$, $N = p, d$ or a nucleus, and X the inclusive hadronic final state. The 4-momentum transfers $q^2 = -Q^2$ involved are at least of the order of $Q^2 \geq 4 \text{ GeV}^2$ and one may resolve spatial scales of approximately $1/\sqrt{Q^2}$. The different deep inelastic charged—and neutral current reactions offer complementary sensitivity to unfold the quark flavor and gluonic structure of the nucleons. Furthermore, polarized lepton scattering off polarized targets is studied in order to investigate the spin structure of the nucleons.

The electron–proton experiments performed at SLAC in 1968 [1–6] cf. also [7–9] and at DESY [10–12] found the famous scaling behavior of the structure functions which had been predicted by Bjorken before [13]. These measurements led to the creation of the parton model [14–16]. Several years later, after a series of experiments had confirmed its main predictions, the partons were identified with the quarks, anti-quarks and gluons as real quantum fields, which are confined inside hadrons. Being formerly merely mathematical objects [17, 18] they became essential building blocks of the Standard Model of elementary particle physics, besides the leptons and the electroweak gauge fields, thereby solving the anomaly-problem [19–21].

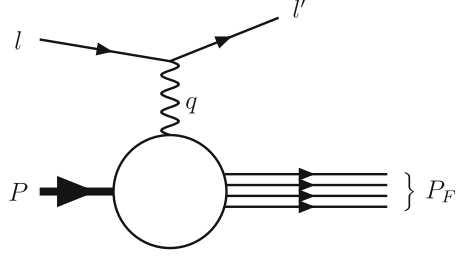
In the following years, more studies were undertaken at higher energies, such as the electron–proton/neutron scattering experiments at SLAC [22–25]. Muons were used as probes of the nucleons by EMC [26, 27] BCDMS [28–32] and NMC [33–35] at the SPS [36] at CERN, as well as by the E26—[37–39] CHIO—[40]

and E665—[41, 42] collaborations at FERMILAB. For a general review of $\mu^\pm N$ -scattering, see [43]. The latter experiments were augmented by several high energy neutrino scattering experiments by the CHARM- and CDHSW-collaborations [44–49] and the WA21/25-experiments [50, 51] at the SPS, and by the CCFR-collaboration [52–54] at FERMILAB. Further results on neutrinos were reported in Refs. [55–62] cf. also [63–67]. The data of these experiments confirmed QCD as the theory describing the strong interactions within hadrons, most notably by the observation of logarithmic scaling violations of the structure functions at higher energies and lower values of x , which had been precisely predicted by theoretical calculations [68–70].

All these experiments had in common that they were fixed target experiments and therefore could only probe a limited region of phase space, up to $x \geq 10^{-3}$, $Q^2 \leq 500 \text{ GeV}^2$. The first electron–proton collider experiments became possible with the advent of the HERA facility, which began operating in the beginning of the 1990ies at DESY [71]. This allowed measurements at much larger values of Q^2 and at far smaller values of x than before, $x \geq 10^{-4}$, $Q^2 \leq 20.000 \text{ GeV}^2$. The physics potential for the deep–inelastic experiments at HERA was studied during a series of workshops, see [72–80]. HERA collected a vast amount of data until its shutdown in 2007, a part of which is still being analyzed, reaching unprecedented experimental precisions below the level of 1%. Two general purpose experiments to study inclusive and various semi-inclusive unpolarized deep–inelastic reactions, H1 [81] and ZEUS [82] were performed. Both experiments measured the structure functions $F_{2,L}(x, Q^2)$ as well as the heavy quark contributions to these structure functions to high precision. The theoretical calculations in this thesis are important for the analysis and understanding of the latter, as will be outlined in Chap. 3. The HERMES—experiment [83] studied scattering of polarized electrons and positrons off polarized gas—targets. HERA-B [84] was dedicated to the study of CP—violations in the B -sector.

In the following, we give a brief introduction into the theory of DIS and the theoretical tools which are used to predict the properties of structure functions, such as asymptotic scaling and scaling violations. In Sect. 2.1, we discuss the kinematics of the DIS process and derive the cross section for unpolarized electromagnetic electron–proton scattering. In Sect. 2.2, we give a description of the naive parton model, which was employed to explain the results obtained at SLAC and gave a first correct qualitative prediction of the observed experimental data. A rigorous treatment of DIS can be obtained by applying the light-cone expansion to the forward Compton amplitude [85–88] which is described in Sect. 2.3 This is equivalent to the QCD–improved parton model at the level of twist $\tau = 2$, cf. e.g. [89–93]. One obtains evolution equations for the structure functions and the parton densities with respect to the mass scales considered. The evolution is governed by the splitting functions [94] or the anomalous dimensions [68–70] cf. Sect. 2.4.

Fig. 2.1 Schematic graph of deeply inelastic scattering for single boson exchange



2.1 Kinematics and Cross Section

The schematic diagram for the Born cross section of DIS is shown in Fig. 2.1 for single gauge boson exchange. A lepton with momentum l scatters off a nucleon of mass M and momentum P via the exchange of a virtual vector boson with momentum q . The momenta of the outgoing lepton and the set of hadrons are given by l' and P_F , respectively. Here F can consist of any combination of hadronic final states allowed by quantum number conservation. We consider inclusive final states and thus all the hadronic states contributing to F are summed over. The kinematics of the process can be measured from the scattered lepton or the hadronic final states, cf. e.g. [95–97] depending on the respective experiment. The virtual vector boson has space-like momentum with a virtuality Q^2

$$Q^2 \equiv -q^2, \quad q = l - l'. \quad (2.4)$$

There are two additional independent kinematic variables for which we choose

$$s \equiv (P + l)^2, \quad (2.5)$$

$$W^2 \equiv (P + q)^2 = P_F^2. \quad (2.6)$$

Here, s is the total cms energy squared and W denotes the invariant mass of the hadronic final state. In order to describe the process, one usually refers to Bjorken's scaling variable x , the inelasticity y , and the total energy transfer ν of the lepton to the nucleon in the nucleon's rest frame [98]. They are defined by

$$\nu \equiv \frac{P \cdot q}{M} = \frac{W^2 + Q^2 - M^2}{2M}, \quad (2.7)$$

$$x \equiv \frac{-q^2}{2P \cdot q} = \frac{Q^2}{2M\nu} = \frac{Q^2}{W^2 + Q^2 - M^2}, \quad (2.8)$$

$$y \equiv \frac{P \cdot q}{P \cdot l} = \frac{2M\nu}{s - M^2} = \frac{W^2 + Q^2 - M^2}{s - M^2}, \quad (2.9)$$

where lepton masses are disregarded. In general, the virtual vector boson exchanged can be a γ , Z or W^\pm -boson with the in—and outgoing lepton, respectively, being an electron, muon or neutrino. In the following, we consider only unpolarized neutral current charged lepton–nucleon scattering. In addition, we will disregard weak gauge boson effects caused by the exchange of a Z -boson. This is justified as long as the virtuality is not too large, i.e. $Q^2 < 500 \text{ GeV}^2$, cf. [99]. We assume the QED- and electroweak radiative corrections to have been carried out [96, 97, 100].

The kinematic region of DIS is limited by a series of conditions. The hadronic mass obeys

$$W^2 \geq M^2. \quad (2.10)$$

Furthermore,

$$v \geq 0, \quad 0 \leq y \leq 1, \quad s \geq M^2. \quad (2.11)$$

From (2.10) follows the kinematic region for Bjorken- x via

$$W^2 = (P + q)^2 = M^2 - Q^2 \left(1 - \frac{1}{x}\right) \geq M^2 \implies 0 \leq x \leq 1. \quad (2.12)$$

Note that $x = 1$ describes the elastic process, while the inelastic region is defined by $x < 1$. Additional kinematic constraints follow from the design parameters of the accelerator [101, 102]. In the case of HERA, these were 820(920) GeV for the proton beam and 27.5 GeV for the electron beam, resulting in a cms-energy \sqrt{s} of 300.3(319) GeV.¹ This additionally imposes kinematic constraints which follow from

$$Q^2 = xy(s - M^2), \quad (2.13)$$

correlating s and Q^2 . For the kinematics at HERA, this implies

$$Q^2 \leq sx \approx 10^5 x. \quad (2.14)$$

In order to calculate the cross section of deeply inelastic ep -scattering, one considers the tree-level transition matrix element for the electromagnetic current. It is given by, cf. e.g. [89–91]

$$M_{fi} = e^2 \bar{u}(l', \eta') \gamma^\mu u(l, \eta) \frac{1}{q^2} \langle P_F | J_\mu^{em}(0) | P, \sigma \rangle. \quad (2.15)$$

Here, the spin of the charged lepton or nucleon is denoted by $\eta(\eta')$ and σ , respectively. The state vectors of the initial-state nucleons and the hadronic final state are

¹ During the final running period of HERA, low-energy measurements were carried out with $E_p = 460(575) \text{ GeV}$ in order to extract the longitudinal structure function $F_L(x, Q^2)$, [103].

$|P, \sigma\rangle$ and $|P_F\rangle$. The Dirac-matrices are denoted by γ_μ and bi-spinors by u , see Appendix A. Further e is the electric unit charge and $J_\mu^{em}(\xi)$ the quarkonic part of the electromagnetic current operator, which is self-adjoint :

$$J_\mu^\dagger(\xi) = J_\mu(\xi). \quad (2.16)$$

In QCD, it is given by

$$J_\mu^{em}(\xi) = \sum_{f, f'} \bar{\Psi}_f(\xi) \gamma_\mu \lambda_{ff'}^{em} \Psi_{f'}(\xi), \quad (2.17)$$

where $\Psi_f(\xi)$ denotes the quark field of flavor f . For three light flavors, λ^{em} is given by the following combination of Gell–Mann matrices of the flavor group $SU(3)_{flavor}$, cf. [104, 105]

$$\lambda^{em} = \frac{1}{2} \left(\lambda_{flavor}^3 + \frac{1}{\sqrt{3}} \lambda_{flavor}^8 \right). \quad (2.18)$$

According to standard definitions [89–91, 106] the differential inclusive cross section is then given by

$$l'_0 \frac{d\sigma}{d^3l'} = \frac{1}{32(2\pi)^3(l \cdot P)} \sum_{\eta', \eta, \sigma, F} (2\pi)^4 \delta^4(P_F + l' - P - l) |M_{fi}|^2. \quad (2.19)$$

Inserting the transition matrix element (2.15) into the relation for the scattering cross section (2.19), one notices that the trace over the leptonic states forms a separate tensor, $L^{\mu\nu}$. Similarly, the hadronic tensor $W_{\mu\nu}$ is obtained,

$$L_{\mu\nu}(l, l') = \sum_{\eta', \eta} [\bar{u}(l', \eta') \gamma^\mu u(l, \eta)]^* [\bar{u}(l', \eta') \gamma^\nu u(l, \eta)], \quad (2.20)$$

$$W_{\mu\nu}(q, P) = \frac{1}{4\pi} \sum_{\sigma, F} (2\pi)^4 \delta^4(P_F - q - P) \langle P, \sigma | J_\mu^{em}(0) | P_F \rangle \langle P_F | J_\nu^{em}(0) | P, \sigma \rangle. \quad (2.21)$$

Thus one arrives at the following relation for the cross section

$$l'_0 \frac{d\sigma}{d^3l'} = \frac{1}{4P \cdot l} \frac{\alpha^2}{Q^4} L^{\mu\nu} W_{\mu\nu} = \frac{1}{2(s - M^2)} \frac{\alpha^2}{Q^4} L^{\mu\nu} W_{\mu\nu}, \quad (2.22)$$

where α denotes the fine-structure constant, see Appendix A. The leptonic tensor in (2.22) can be easily computed in the context of the Standard Model,

$$L_{\mu\nu}(l, l') = \text{Tr}[\not{l} \gamma^\mu \not{l}' \gamma^\nu] = 4 \left(l_\mu l'_\nu + l'_\mu l_\nu - \frac{Q^2}{2} g_{\mu\nu} \right). \quad (2.23)$$

This is not the case for the hadronic tensor, which contains non-perturbative hadronic contributions due to long-distance effects. To calculate these effects a priori, non-perturbative QCD calculations have to be performed, as in QCD lattice simulations. During the last years these calculations were performed with increasing systematic and numerical accuracy, cf. e.g. [107–111].

The general structure of the hadronic tensor can be fixed using S -matrix theory and the global symmetries of the process. In order to obtain a form suitable for the subsequent calculations, one rewrites Eq. 2.21 as, cf. [90, 112]

$$\begin{aligned} W_{\mu\nu}(q, P) &= \frac{1}{4\pi} \sum_{\sigma} \int d^4\xi \exp(iq\xi) \langle P | [J_{\mu}^{em}(\xi), J_{\nu}^{em}(0)] | P \rangle \\ &= \frac{1}{2\pi} \int d^4\xi \exp(iq\xi) \langle P | [J_{\mu}^{em}(\xi), J_{\nu}^{em}(0)] | P \rangle. \end{aligned} \quad (2.24)$$

Here, the following notation for the spin-average is introduced in Eq. 2.24

$$\frac{1}{2} \sum_{\sigma} \langle P, \sigma | X | P, \sigma \rangle \equiv \langle P | X | P \rangle. \quad (2.25)$$

Further, $[a, b]$ denotes the commutator of a and b . Using symmetry and conservation laws, the hadronic tensor can be decomposed into different scalar structure functions and thus be stripped of its Lorentz-structure. In the most general case, including polarization, there are 14 independent structure functions [113, 114] which contain all information on the structure of the proton. However, in the case considered here, only two structure functions contribute. One uses Lorentz- and time-reversal invariance [85–88] and additionally the fact that the electromagnetic current is conserved. This enforces electromagnetic gauge invariance for the hadronic tensor,

$$q_{\mu} W^{\mu\nu} = 0. \quad (2.26)$$

The leptonic tensor (2.23) is symmetric and thus $W_{\mu\nu}$ can be taken to be symmetric as well, since all antisymmetric parts are canceled in the contraction. By making a general ansatz for the hadronic tensor using these properties, one obtains

$$\begin{aligned} W_{\mu\nu}(q, P) &= \frac{1}{2x} \left(g_{\mu\nu} + \frac{q_{\mu}q_{\nu}}{Q^2} \right) F_L(x, Q^2) \\ &+ \frac{2x}{Q^2} \left(P_{\mu}P_{\nu} + \frac{q_{\mu}P_{\nu} + q_{\nu}P_{\mu}}{2x} - \frac{Q^2}{4x^2} g_{\mu\nu} \right) F_2(x, Q^2). \end{aligned} \quad (2.27)$$

The dimensionless structure functions $F_2(x, Q^2)$ and $F_L(x, Q^2)$ depend on two variables, Bjorken- x and Q^2 , contrary to the case of elastic scattering, in which only one variable, e.g. Q^2 , determines the cross section. Due to hermiticity of the hadronic tensor, the structure functions are real. The decomposition (2.27) of the hadronic tensor leads to the differential cross section of unpolarized DIS in case of single photon exchange

$$\frac{d\sigma}{dx dy} = \frac{2\pi\alpha^2}{xyQ^2} \left\{ \left[1 + (1-y)^2 \right] F_2(x, Q^2) - y^2 F_L(x, Q^2) \right\}. \quad (2.28)$$

A third structure function, $F_1(x, Q^2)$,

$$F_1(x, Q^2) = \frac{1}{2x} \left[F_2(x, Q^2) - F_L(x, Q^2) \right], \quad (2.29)$$

which is often found in the literature, is not independent of the previous ones.

For completeness, we finally give the full Born cross section for the neutral current, including the exchange of Z -bosons, cf. [97]. Not neglecting the lepton mass m , it is given by

$$\begin{aligned} \frac{d^2\sigma_{\text{NC}}}{dx dy} = \frac{2\pi\alpha^2}{xyQ^2} \left\{ \left[2(1-y) - 2xy \frac{M^2}{s} + \left(1 - 2 \frac{m^2}{Q^2} \right) \left(1 + 4x^2 \frac{M^2}{Q^2} \right) \right. \right. \\ \left. \left. \times \frac{y^2}{1 + R(x, Q^2)} \right] \mathcal{F}_2(x, Q^2) + xy(2-y) \mathcal{F}_3(x, Q^2) \right\}. \end{aligned} \quad (2.30)$$

Here, $R(x, Q^2)$ denotes the ratio

$$R(x, Q^2) = \frac{\sigma_L}{\sigma_T} = \left(1 + 4x^2 \frac{M^2}{Q^2} \right) \frac{\mathcal{F}_2(x, Q^2)}{2x \mathcal{F}_1(x, Q^2)} - 1, \quad (2.31)$$

and the **effective** structure functions $\mathcal{F}_l(x, Q^2)$, $l = 1, \dots, 3$ are represented by the structure functions F_l , G_l and H_l via

$$\begin{aligned} \mathcal{F}_{1,2}(x, Q^2) = F_{1,2}(x, Q^2) + 2|Q_e| (v_e + \lambda a_e) \chi(Q^2) G_{1,2}(x, Q^2) \\ + 4 \left(v_e^2 + a_e^2 + 2\lambda v_e a_e \right) \chi^2(Q^2) H_{1,2}(x, Q^2), \end{aligned} \quad (2.32)$$

$$\begin{aligned} x \mathcal{F}_3(x, Q^2) = -2 \text{sign}(Q_e) \left\{ |Q_e| (a_e + \lambda v_e) \chi(Q^2) x G_3(x, Q^2) \right. \\ \left. + \left[2v_e a_e + \lambda (v_e^2 + a_e^2) \right] \chi^2(Q^2) x H_3(x, Q^2) \right\}. \end{aligned} \quad (2.33)$$

Here, $Q_e = -1$, $a_e = 1$ in case of electrons and

$$\lambda = \xi \text{sign}(Q_e), \quad (2.34)$$

$$v_e = 1 - 4 \sin^2 \theta_W^{\text{eff}}, \quad (2.35)$$

$$\chi(Q^2) = \frac{G_\mu}{\sqrt{2}} \frac{M_Z^2}{8\pi\alpha(Q^2)} \frac{Q^2}{Q^2 + M_Z^2}, \quad (2.36)$$

with ξ the electron polarization, θ_W^{eff} the effective weak mixing angle, G_μ the Fermi constant and M_Z the Z -boson mass.

2.2 The Parton Model

The structure functions (2.27) depend on two kinematic variables, x and Q^2 . Based on an analysis using current algebra, Bjorken predicted scaling of the structure functions, cf. [13]

$$\lim_{\{Q^2, \nu\} \rightarrow \infty, x=\text{const.}} F_{(2,L)}(x, Q^2) = F_{(2,L)}(x) . \quad (2.37)$$

This means that in the Bjorken limit $\{Q^2, \nu\} \rightarrow \infty$, with x fixed, the structure functions depend on the ratio Q^2/ν only. Soon after this prediction, approximate scaling was observed experimentally in electron-proton collisions at SLAC (1968) [3–6] cf. also [7–9].² Similar to the α –particle scattering experiments by Rutherford in 1911 [115] the cross section remained large at high momentum transfer Q^2 , a behavior which is known from point-like targets. This was found in contradiction to the expectation that the cross section should decrease rapidly with increasing Q^2 , since the size of the proton had been determined to be about 10^{-13} cm with a smooth charge distribution [116–118]. However, only in rare cases a single proton was detected in the final state, instead it consisted of a large number of hadrons. A proposal by Feynman contained the correct ansatz. To account for the observations, he introduced the parton model [14, 15] cf. also [16, 89, 91–93, 119]. He assumed the proton as an extended object, consisting of several point-like particles, the partons. They are bound together by their mutual interaction and behave like free particles during the interaction with the highly virtual photon in the Bjorken-limit.³ One arrives at the picture of the proton being “frozen” while the scattering takes place. The electron scatters elastically off the partons and this process does not interfere with the other partonic states, the “spectators”. The DIS cross section is then given by the incoherent sum over the individual virtual electron–parton cross sections. Since no information on the particular proton structure is known, Feynman described parton i by the parton distribution function (PDF) $f_i(z)$. It gives the probability to find parton i in the “frozen” proton, carrying the fraction z of its momentum. Fig 2.2 shows a schematic picture of the parton model in Born approximation. The in- and out-going parton momenta are denoted by p and p' , respectively.

Similar to the scaling variable x , one defines the partonic scaling variable τ ,

$$\tau \equiv \frac{Q^2}{2p \cdot q} . \quad (2.38)$$

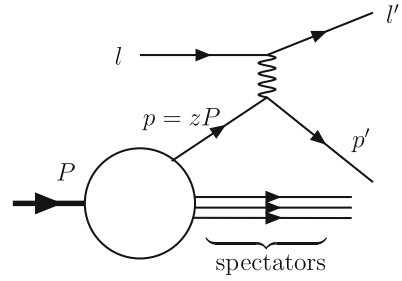
It plays the same role as the Bjorken-variable, but for the partonic sub-process. In the collinear parton model,⁴ which is applied throughout this thesis, $p = zP$ holds,

² The results obtained at DESY [10–12] pointed in the same direction, but were less decisive, because not as large values of Q^2 as at SLAC could be reached.

³ Asymptotic freedom, which was discovered later, is instrumental for this property.

⁴ For other parton models, as the covariant parton model, cf. [120–125].

Fig. 2.2 Deeply inelastic electron–proton scattering in the parton model



i.e., the momentum of the partons is taken to be collinear to the proton momentum. From (2.38) one obtains

$$\tau z = x . \quad (2.39)$$

Feynman's original parton model, referred to as the naive parton model, neglects the mass of the partons and enforces the strict correlation

$$\delta \left(\frac{q \cdot p}{M} - \frac{Q^2}{2M} \right), \quad (2.40)$$

due to the experimentally observed scaling behavior, which leads to $z = x$. The naive parton model then assumes, in accordance with the quark hypothesis [16–18] that the proton is made up of three valence quarks, two up and one down type, cf. e.g. [126]. This conclusion was generally accepted only several years after the introduction of the parton model, when various experiments had verified its predictions.

Let us consider a simple example, which reproduces the naive parton model at LO and incorporates already some aspects of the improved parton model. The latter allows virtual quark states (sea-quarks) and gluons as partons as well. In the QCD-improved parton model, cf. [89, 91,–93] besides the δ -distribution, (2.40), a function $\mathcal{W}_{\mu\nu}^i(\tau, Q^2)$ contributes to the hadronic tensor. It is called partonic tensor and given by the hadronic tensor, Eq. 2.24, replacing the hadronic states by partonic states i . The basic assumption is that the hadronic tensor can be factorized into the PDFs and the partonic tensor, cf. e.g. [127–134]. The PDFs are non-perturbative quantities and have to be extracted from experiment, whereas the partonic tensors are calculable perturbatively. A more detailed discussion of this using the LCE is given in Sect. 2.3. The hadronic tensor reads, cf. [135]

$$W_{\mu\nu}(x, Q^2) = \frac{1}{4\pi} \sum_i \int_0^1 dz \int_0^1 d\tau (f_i(z) + f_{\bar{i}}(z)) \mathcal{W}_{\mu\nu}^i(\tau, Q^2) \delta(x - z\tau) . \quad (2.41)$$

Here, the number of partons and their respective type are not yet specified and we have included the corresponding PDF of the respective anti-parton, denoted by $f_{\bar{i}}(z)$. Let us assume that the electromagnetic parton current takes the simple form

$$\langle i | j_\mu^i(\tau) | i \rangle = -i e_i \bar{u}^i \gamma_\mu u^i, \quad (2.42)$$

similar to the leptonic current (2.15). Here e_i is the electric charge of parton i . At LO one finds

$$\mathcal{W}_{\mu\nu}^i(\tau, Q^2) = \frac{2\pi e_i^2}{q \cdot p^i} \delta(1 - \tau) \left[2p_\mu^i p_\nu^i + p_\mu^i q_\nu + p_\nu^i q_\mu - g_{\mu\nu} q \cdot p^i \right]. \quad (2.43)$$

The δ -distribution in (2.43), together with the δ -distribution in (2.41), just reproduces Feynman's assumption of the naive parton model, $z = x$. Substitution of (2.43) into the general expression for the hadronic tensor (2.27) and projecting onto the structure functions yields

$$\begin{aligned} F_L(x, Q^2) &= 0, \\ F_2(x, Q^2) &= x \sum_i e_i^2 (f_i(x) + f_{\bar{i}}(x)). \end{aligned} \quad (2.44)$$

This result, at LO, is the same as in the naive parton model. It predicts

- the Callan–Gross relation, cf. [136]

$$F_L(x, Q^2) = F_2(x, Q^2) - 2x F_1(x, Q^2) = 0. \quad (2.45)$$

- the structure functions are scale-independent.

These findings were a success of the parton model, since they reproduced the general behavior of the data as observed by the MIT/SLAC experiments.

Finally, we present for completeness the remaining structure functions $G_{2,3}$ and $H_{2,3}$ at the Born level for the complete neutral current, cf. Eq. (2.30),

$$G_2(x, Q^2) = x \sum_i |e_i| v_i (f_i(x) + f_{\bar{i}}(x)), \quad (2.46)$$

$$H_2(x, Q^2) = x \sum_i \frac{1}{4} (v_i^2 + a_i^2) (f_i(x) + f_{\bar{i}}(x)), \quad (2.47)$$

$$x G_3(x, Q^2) = x \sum_i |e_i| a_i (f_i(x) - f_{\bar{i}}(x)), \quad (2.48)$$

$$x H_3(x, Q^2) = x \sum_i \frac{1}{2} v_i a_i (f_i(x) - f_{\bar{i}}(x)), \quad (2.49)$$

with $a_i = 1$ and

$$v_i = 1 - 4|e_i| \sin^2 \theta_W^{\text{eff}}. \quad (2.50)$$

2.2.1 Validity of the Parton Model

The validity of the parton picture can be justified by considering an impulse approximation of the scattering process as seen from a certain class of reference frames, in which the proton momentum is taken to be very large (P_∞ -frames). Two things happen to the proton when combining this limit with the Bjorken-limit: The internal interactions of its partons are time dilated, and it is Lorentz contracted in the direction of the collision. As the cms energy increases, the parton lifetimes are lengthened and the time it takes the electron to interact with the proton is shortened. Therefore the condition for the validity of the parton model is given by, cf. [16, 137]

$$\frac{\tau_{\text{int}}}{\tau_{\text{life}}} \ll 1. \quad (2.51)$$

Here τ_{int} denotes the interaction time and τ_{life} the average life time of a parton. If (2.51) holds, the proton will be in a single virtual state characterized by a certain number of partons during the entire interaction time. This justifies the assumption that parton i carries a definite momentum fraction z_i , $0 \leq z_i \leq 1$, of the proton in the cms. This parton model is also referred to as collinear parton model, since the proton is assumed to consist out of a stream of partons with parallel momenta. Further $\sum_i z_i = 1$ holds. In order to derive the fraction of times in (2.51), one aligns the coordinate system parallel to the proton's momentum. Thus one obtains in the limit $P_3^2 \gg M^2$, [138]

$$P = \left(\sqrt{P_3^2 + M^2}; 0, 0, P_3 \right) \approx \left(P_3 + \frac{M^2}{2 \cdot P_3}; 0, 0, P_3 \right). \quad (2.52)$$

The photon momentum can be parametrized by

$$q = (q_0; q_3, \vec{q}_\perp), \quad (2.53)$$

where \vec{q}_\perp denotes its transverse momentum with respect to the proton. By choosing the cms of the initial states as reference and requiring that νM and q^2 approach a limit independent of P_3 as $P_3 \rightarrow \infty$, one finds for the characteristic interaction time scale, using an (approximate) time-energy uncertainty relation,

$$\tau_{\text{int}} \simeq \frac{1}{q_0} = \frac{4P_3x}{Q^2(1-x)}. \quad (2.54)$$

The life time of the individual partons is estimated accordingly to be inversely proportional to the energy fluctuations of the partons around the average energy E

$$\tau_{\text{life}} \simeq \frac{1}{\sum_i E_i - E}. \quad (2.55)$$

Here E_i denote the energies of the individual partons. After introducing the two-momentum $\vec{k}_{\perp i}$ of the partons perpendicular to the direction of motion of the proton as given in (2.52), a simple calculation yields, cf. [138]

Fig. 2.3 Schematic picture of the optical theorem

$$\left| \sum_F \left[\text{Diagram} \right] \right|^2 = \frac{1}{\pi} \text{Im} \left[\text{Diagram} \right]$$

$$\frac{\tau_{\text{int}}}{\tau_{\text{life}}} = \frac{2x}{Q^2(1-x)} \left(\sum_i \frac{(m_i^2 + k_{\perp i}^2)}{z_i} - M^2 \right), \quad (2.56)$$

where m_i denotes the mass of the i th parton. This expression is independent of P_3 . The above procedure allows therefore to estimate the probability of deeply inelastic scattering to occur independently of the large momentum of the proton. Accordingly, we consider now the case of two partons with momentum fractions x and $1-x$ and equal perpendicular momentum, neglecting all masses. One obtains

$$\frac{\tau_{\text{int}}}{\tau_{\text{life}}} \approx \frac{2k_{\perp}^2}{Q^2(1-x)^2}. \quad (2.57)$$

This example leads to the conclusion, that deeply inelastic scattering probes single partons if the virtuality of the photon is much larger than the transverse momenta squared of the partons and Bjorken- x is neither close to one nor zero. In the latter case, xP_3 would be the large momentum to be considered. If one does not neglect the quark masses, one has to adjust this picture, as will be described in [Sect. 3.3](#).

2.3 The Light-Cone Expansion

In quantum field theory one usually considers time-ordered products, denoted by T , rather than a commutator as it appears in the hadronic tensor in [Eq. 2.24](#). The hadronic tensor can be expressed as the imaginary part of the forward Compton amplitude for virtual gauge boson–nucleon scattering, $T_{\mu\nu}(q, P)$. The optical theorem, depicted graphically in [Fig. 2.3](#), yields

$$W_{\mu\nu}(q, P) = \frac{1}{\pi} \text{Im} T_{\mu\nu}(q, P), \quad (2.58)$$

where the Compton amplitude is given by cf. [\[104\]](#)

$$T_{\mu\nu}(q, P) = i \int d^4\xi \exp(iq\xi) \langle P | T J_{\mu}(\xi) J_{\nu}(0) | P \rangle. \quad (2.59)$$

By applying the same invariance and conservation conditions as for the hadronic tensor, the Compton amplitude can be expressed in the unpolarized case by two amplitudes $T_L(x, Q^2)$ and $T_2(x, Q^2)$. It is then given by

$$\begin{aligned}
T_{\mu\nu}(q, P) = & \frac{1}{2x} \left(g_{\mu\nu} + \frac{q_\mu q_\nu}{Q^2} \right) T_L(x, Q^2) \\
& + \frac{2x}{Q^2} \left(P_\mu P_\nu + \frac{q_\mu P_\nu + q_\nu P_\mu}{2x} - \frac{Q^2}{4x^2} g_{\mu\nu} \right) T_2(x, Q^2) .
\end{aligned} \tag{2.60}$$

Using translation invariance, one can show that (2.59) is crossing symmetric under $q \rightarrow -q$, cf. [113, 139]

$$T_{\mu\nu}(q, P) = T_{\mu\nu}(-q, P), \tag{2.61}$$

with $q \rightarrow -q$ being equivalent to $\nu, x \rightarrow (-\nu), (-x)$. The corresponding relations for the amplitudes are then obtained by considering (2.60)

$$T_{(2,L)}(x, Q^2) = T_{(2,L)}(-x, Q^2) . \tag{2.62}$$

By (2.58) these amplitudes relate to the structure functions F_L and F_2 as

$$F_{(2,L)}(x, Q^2) = \frac{1}{\pi} \text{Im } T_{(2,L)}(x, Q^2) . \tag{2.63}$$

Another general property of the Compton amplitude is that T_L and T_2 are real analytic functions of x at fixed Q^2 , cf. [140] i.e.

$$T_{(2,L)}(x^*, Q^2) = T_{(2,L)}^*(x, Q^2) . \tag{2.64}$$

Using this description one can perform the LCE [85–88] or the cut—vertex method in the time—like case [141–143] respectively, and derive general properties of the moments of the structure functions as will be shown in the subsequent Section. A technical aspect which has been proved very useful is to work in Mellin space rather than in x -space. The N th Mellin moment of a function f is defined through the integral

$$\mathbf{M}[f](N) \equiv \int_0^1 dz z^{N-1} f(z) . \tag{2.65}$$

This transform diagonalizes the Mellin-convolution $f \otimes g$ of two functions f, g

$$[f \otimes g](z) = \int_0^1 dz_1 \int_0^1 dz_2 \delta(z - z_1 z_2) f(z_1) g(z_2) . \tag{2.66}$$

The convolution (2.66) decomposes into a simple product of the Mellin-transforms of the two functions,

$$\mathbf{M}[f \otimes g](N) = \mathbf{M}[f](N) \mathbf{M}[g](N) . \tag{2.67}$$

In Eqs. 2.65, 2.67 N is taken to be an integer. However, later on one may perform an analytic continuation to arbitrary complex values of N [144, 145]. Note that it is enough to know all even or odd integer moments—as is the case for inclusive DIS—of the functions f , g to perform an analytic continuation to arbitrary complex values $N \in \mathbb{C}$, [146, 147]. Then Eq. 2.66 can be obtained from the relation for the moments (2.67) by an inverse Mellin–transform. Hence in this case the z - and N -space description are equivalent, which we will frequently use later on.

2.3.1 Light–Cone Dominance

It can be shown that in the Bjorken limit, $Q^2 \rightarrow \infty$, $\nu \rightarrow \infty$, x fixed, the hadronic tensor is dominated by its contribution near the light–cone, i.e. by the values of the integrand in (2.24) at $\xi^2 \approx 0$, cf. [85–88]. This can be understood by considering the infinite momentum frame, see Sect. 2.2.1,

$$P = (P_3; 0, 0, P_3), \quad (2.68)$$

$$q = \left(\frac{\nu}{2P_3}; \sqrt{Q^2}, 0, \frac{-\nu}{2P_3} \right), \quad (2.69)$$

$$P_3 \approx \sqrt{\nu} \rightarrow \infty. \quad (2.70)$$

According to the Riemann–Lebesgue theorem, the integral in (2.24) is dominated by the region where $q \cdot \xi \approx 0$ due to the rapidly oscillating exponential $\exp(iq \cdot \xi)$, [89]. One can now rewrite the dot product as, cf. [105]

$$q \cdot \xi = \frac{1}{2}(q^0 - q^3)(\xi^0 + \xi^3) + \frac{1}{2}(q^0 + q^3)(\xi^0 - \xi^3) - q^1 \xi^1, \quad (2.71)$$

and infer that the condition $q \cdot \xi \approx 0$ in the Bjorken-limit is equivalent to

$$\xi^0 \pm \xi^3 \propto \frac{1}{\sqrt{\nu}}, \quad \xi^1 \propto \frac{1}{\sqrt{\nu}}, \quad (2.72)$$

which results in

$$\xi^2 \approx 0, \quad (2.73)$$

called **light–cone dominance**: for DIS in the Bjorken-limit the dominant contribution to the hadronic tensor $W_{\mu\nu}(q, P)$ and the Compton Amplitude comes from the region where $\xi^2 \approx 0$.

This property allows to apply the LCE of the current–current correlation in Eq. 2.24 and for the time ordered product in Eq. 2.59, respectively. In the latter case it reads for scalar currents, cf. [85–88]

$$\lim_{\xi^2 \rightarrow 0} \mathbb{T}J(\xi), J(0) \propto \sum_{i,N,\tau} \bar{C}_{i,\tau}^N(\xi^2, \mu^2) \xi_{\mu_1} \dots \xi_{\mu_N} O_{i,\tau}^{\mu_1 \dots \mu_N}(0, \mu^2). \quad (2.74)$$

The $O_{i,\tau}(\xi, \mu^2)$ are local operators which are finite as $\xi^2 \rightarrow 0$. The singularities which appear for the product of two operators as their arguments become equal are shifted to the c -number coefficients $\bar{C}_{i,\tau}^N(\xi^2, \mu^2)$, the Wilson coefficients, and can therefore be treated separately. In Eq. 2.74, μ^2 is the factorization scale describing at which point the separation between the perturbative and non-perturbative contributions takes place. The summation index i runs over the set of allowed operators in the model, while the sum over N extends to infinity. Dimensional analysis shows that the degree of divergence of the functions $\bar{C}_{i,\tau}^N$ as $\xi^2 \rightarrow 0$ is given by

$$\bar{C}_{i,\tau}^N(\xi^2, \mu^2) \propto \left(\frac{1}{\xi^2} \right)^{-\tau/2 + d_J}. \quad (2.75)$$

Here, d_J denotes the canonical dimension of the current $J(\xi)$ and τ is the twist of the local operator $O_{i,\tau}^{\mu_1 \dots \mu_N}(\xi, \mu^2)$, which is defined by, cf. [148]

$$\tau \equiv D_O - N. \quad (2.76)$$

D_O is the canonical (mass) dimension of $O_{i,\tau}^{\mu_1 \dots \mu_N}(\xi, \mu^2)$ and N is called its spin. From (2.75) one can infer that the most singular coefficients are those related to the operators of lowest twist, i.e. in the case of the LCE of the electromagnetic current (2.17), twist $\tau = 2$. The contributions due to higher twist operators are suppressed by factors of $(\bar{\mu}^2/Q^2)^k$, with $\bar{\mu}$ a typical hadronic mass scale of $O(1 \text{ GeV})$. In a wide range of phase-space it is thus sufficient to consider the leading twist contributions only, which we will do in the following and omit the index τ .

2.3.2 A Simple Example

In this Section, we consider a simple example of the LCE applied to the Compton amplitude and its relation to the hadronic tensor, neglecting all Lorentz-indices and model dependence, cf. Refs. [90, 149]. The generalization to the case of QCD is straightforward and hence we will already make some physical arguments which apply in both cases. The scalar expressions corresponding to the hadronic tensor and the Compton amplitude are given by

$$W(x, Q^2) = \frac{1}{2\pi} \int d^4\xi \exp(iq\xi) \langle P | [J(\xi), J(0)] | P \rangle, \quad (2.77)$$

$$T(x, Q^2) = i \int d^4\xi \exp(iq\xi) \langle P | \mathbb{T}J(\xi) J(0) | P \rangle. \quad (2.78)$$

Eq. 2.78 can be evaluated in the limit $\xi^2 \rightarrow 0$ for twist $\tau = 2$ by using the LCE given in Eq. 2.74, where for brevity only one local operator is considered. The coefficient functions in momentum space are defined as

$$\int \exp(iq \cdot \xi) \xi_{\mu_1} \dots \xi_{\mu_N} \bar{C}^N(\xi^2, \mu^2) \equiv -i \left(\frac{2}{-q^2} \right)^N q_{\mu_1} \dots q_{\mu_N} C^N \left(\frac{Q^2}{\mu^2} \right). \quad (2.79)$$

The nucleon states act on the composite operators only and the corresponding matrix elements can be expressed as

$$\langle P | O^{\mu_1 \dots \mu_N}(0, \mu^2) | P \rangle = A^N \left(\frac{P^2}{\mu^2} \right) P^{\mu_1} \dots P^{\mu_N} + \text{trace terms}. \quad (2.80)$$

The trace terms in the above equation can be neglected, because due to dimensional counting they would give contributions of the order $1/Q^2$, $1/\nu$ and hence are irrelevant in the Bjorken-limit. Thus the Compton amplitude reads cf. e.g. [90, 91]

$$T(x', Q^2) = 2 \sum_{N=0,2,4,\dots} C^N \left(\frac{Q^2}{\mu^2} \right) A^N \left(\frac{P^2}{\mu^2} \right) x'^N, \quad x' = \frac{1}{x} \quad (2.81)$$

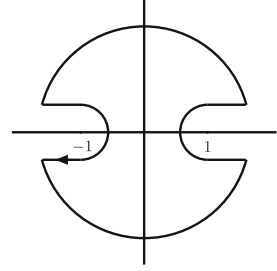
In (2.81) only the even moments contribute. This is a consequence of crossing symmetry, Eq. 2.62, and holds as well in the general case of unpolarized DIS for single photon exchange. In other cases the projection is onto the odd moments. Depending on the type of the observable the series may start at different initial values, cf. e.g. [113, 114]. The sum in Eq. 2.81 is convergent in the unphysical region $x \geq 1$ and an analytic continuation to the physical region $0 \leq x \leq 1$ has to be performed. Here, one of the assumptions is that scattering amplitudes are analytic in the complex plane except at values of kinematic variables allowing intermediate states to be on mass-shell. This general feature has been proved to all orders in perturbation theory [150, 151]. In QCD, it is justified on grounds of the parton model. When $\nu \geq Q^2/2M$, i.e. $0 \leq x \leq 1$, the virtual photon-proton system can produce a physical hadronic intermediate state, so the $T_{(2,L)}(x, Q^2)$ and $T(x, Q^2)$, respectively, have cuts along the positive (negative) real x -axis starting from $1(-1)$ and poles at $\nu = Q^2/2M$ ($x = 1, -1$). The discontinuity along the cut is then just given by (2.58). The Compton amplitude can be further analyzed by applying (subtracted) dispersion relations, cf. [113, 114]. Equivalently, one can divide both sides of Eq. 2.81 by x'^m and integrate along the path shown in Fig. 2.4, cf. [90, 135].

For the left-hand side of (2.81) one obtains

$$\frac{1}{2\pi i} \oint dx' \frac{T(x', Q^2)}{x'^m} = \frac{2}{\pi} \int_1^\infty \frac{dx'}{x'^m} \text{Im } T(x', Q^2) = 2 \int_0^1 dx x^{m-2} W(x, Q^2), \quad (2.82)$$

where the optical theorem (2.58) and crossing symmetry (2.62) have been used. The right-hand side of (2.81) yields

Fig. 2.4 Integration contour in the complex x' -plane



$$\frac{1}{\pi i} \sum_{N=0,2,4,\dots} C^N \left(\frac{Q^2}{\mu^2} \right) A^N \left(\frac{P^2}{\mu^2} \right) \oint dx' x'^{N-m} = 2C^{m-1} \left(\frac{Q^2}{\mu^2} \right) A^{m-1} \left(\frac{P^2}{\mu^2} \right). \quad (2.83)$$

Thus from Eqs. 2.82 and 2.83 one obtains for the moments of the scalar hadronic tensor defined in Eq. 2.77

$$\int_0^1 dx x^{N-1} W(x, Q^2) = C^N \left(\frac{Q^2}{\mu^2} \right) A^N \left(\frac{P^2}{\mu^2} \right). \quad (2.84)$$

2.3.3 The Light-Cone Expansion Applied to DIS

In order to derive the moment-decomposition of the structure functions one essentially has to go through the same steps as in the previous section. The LCE of the physical forward Compton amplitude (2.59) at the level of twist $\tau = 2$ in the Bjorken-limit is given by, cf. [149, 152]

$$\begin{aligned} T_{\mu\nu}(q, P) \rightarrow \sum_{i,N} & \left\{ \left[Q^2 g_{\mu\mu_1} g_{\nu\mu_2} + g_{\mu\mu_1} q_\nu q_{\mu_2} + g_{\nu\mu_2} q_\mu q_{\mu_1} - g_{\mu\nu} q_{\mu_1} q_{\mu_2} \right] \right. \\ & \times C_{i,2} \left(N, \frac{Q^2}{\mu^2} \right) + \left[g_{\mu\nu} + \frac{q_\mu q_\nu}{Q^2} \right] q_{\mu_1} q_{\mu_2} C_{i,L} \left(N, \frac{Q^2}{\mu^2} \right) \Big\} \\ & \times q_{\mu_3} \dots q_{\mu_N} \left(\frac{2}{Q^2} \right)^N \langle P | O_i^{\mu_1 \dots \mu_N}(\mu^2) | P \rangle. \end{aligned} \quad (2.85)$$

Additionally to Sect. 2.3.2, the index i runs over the allowed operators which emerge from the expansion of the product of two electromagnetic currents, Eq. 2.17. The possible twist-2 operators are given by⁵ [142]

⁵ Here we consider only the spin-averaged case for single photon exchange. Other operators contribute for parity-violating processes, in the polarized case and for transversity, cf. Chaps. 8 and 9.

$$O_{q,r;\mu_1,\dots,\mu_N}^{NS} = i^{N-1} \mathbf{S} \left[\bar{\psi} \gamma_{\mu_1} D_{\mu_2} \dots D_{\mu_N} \frac{\lambda_r}{2} \psi \right] \text{---trace terms,} \quad (2.86)$$

$$O_{g;\mu_1,\dots,\mu_N}^S = i^{N-1} \mathbf{S} \left[\bar{\psi} \gamma_{\mu_1} D_{\mu_2} \dots D_{\mu_N} \psi \right] \text{---trace terms,} \quad (2.87)$$

$$O_{g;\mu_1,\dots,\mu_N}^S = 2i^{N-2} \mathbf{S} \mathbf{Sp} \left[F_{\mu_1\alpha}^a D_{\mu_2} \dots D_{\mu_{N-1}} F_{\mu_N}^{\alpha,a} \right] \text{---trace terms.} \quad (2.88)$$

Here, \mathbf{S} denotes the symmetrization operator of the Lorentz indices μ_1, \dots, μ_N . λ_r is the flavor matrix of $SU(n_f)$ with n_f light flavors, ψ denotes the quark field, $F_{\mu\nu}^a$ the gluon field-strength tensor, and D_μ the covariant derivative. The indices q, g represent the quark- and gluon-operator, respectively. \mathbf{Sp} in (2.88) is the color-trace and a the color index in the adjoint representation, cf. Appendix A. The quark-fields carry color indices in the fundamental representation, which have been suppressed. The classification of the composite operators (2.86–2.88) in terms of flavor singlet (S) and non-singlet (NS) refers to their symmetry properties with respect to the flavor group $SU(n_f)$. The operator in Eq. 2.86 belongs to the adjoint representation of $SU(n_f)$, whereas the operators in Eqs. 2.87, 2.88 are singlets under $SU(n_f)$. Neglecting the trace terms, one rewrites the matrix element of the composite operators in terms of its Lorentz structure and the scalar operator matrix elements, cf. [91, 105]

$$\langle P | O_i^{\mu_1 \dots \mu_N} | P \rangle = A_i \left(N, \frac{P^2}{\mu^2} \right) P^{\mu_1} \dots P^{\mu_N}. \quad (2.89)$$

Eq. 2.85 then becomes

$$\begin{aligned} T_{\mu\nu}(q, P) = 2 \sum_{i,N} \left\{ \frac{2x}{Q^2} \left[P_\mu P_\nu + \frac{P_\mu q_\nu + P_\nu q_\mu}{2x} - \frac{Q^2}{4x^2} g_{\mu\nu} \right] C_{i,2} \left(N, \frac{Q^2}{\mu^2} \right) \right. \\ \left. + \frac{1}{2x} \left[g_{\mu\nu} + \frac{q_\mu q_\nu}{Q^2} \right] C_{i,L} \left(N, \frac{Q^2}{\mu^2} \right) \right\} \\ \times \frac{1}{x^{N-1}} A_i \left(N, \frac{P^2}{\mu^2} \right). \end{aligned} \quad (2.90)$$

Comparing Eq. 2.90 with the general Lorentz structure expected for the Compton amplitude Eq. 2.60, the relations of the scalar forward amplitudes to the Wilson coefficients and nucleon matrix elements can be read off

$$T_{(2,L)}(x, Q^2) = 2 \sum_{i,N} \frac{1}{x^{N-1}} C_{i,(2,L)} \left(N, \frac{Q^2}{\mu^2} \right) A_i \left(N, \frac{P^2}{\mu^2} \right). \quad (2.91)$$

Eq. 2.91 is of the same type as Eq. 2.81 and one thus obtains for the moments of the structure functions

$$F_{(2,L)}(N, Q^2) = \mathbf{M}[F_{(2,L)}(x, Q^2)](N) \quad (2.92)$$

$$= \sum_i C_{i,(2,L)} \left(\frac{Q^2}{\mu^2}, N \right) A_i \left(\frac{P^2}{\mu^2}, N \right). \quad (2.93)$$

The above equations have already been written in Mellin space, which we will always do from now on, if not indicated otherwise. Eqs. 2.91, 2.93 together with the general structure of the Compton amplitude, Eqs. 2.60, 2.90 and the hadronic tensor, Eq. 2.27 are the basic equations for theoretical or phenomenological analysis of DIS in the kinematic regions where higher twist effects can be safely disregarded. Note that the generalization of these equations to electroweak or polarized interactions is straightforward by including additional operators and Wilson coefficients. In order to interpret Eqs. 2.91, 2.93 one uses the fact that the Wilson coefficients $C_{i,(2,L)}$ are independent of the proton state. This is obvious since the wave function of the proton only enters into the definition of the operator matrix elements, cf. Eq. 2.89. In order to calculate the Wilson coefficients, the proton state has therefore to be replaced by a suitably chosen quark or gluon state i with momentum p . The corresponding partonic tensor is denoted by $\mathcal{W}_{\mu\nu}^i(q, p)$, cf. below Eq. 2.40, with scalar amplitudes $\mathcal{F}_{(2,L)}^i(\tau, Q^2)$. Here τ is the partonic scaling variable defined in Eq. 2.38. The LCE of the electromagnetic current does not change and the replacement only affects the operator matrix elements. The forward Compton amplitude for photon–quark (gluon) scattering corresponding to $\mathcal{W}_{\mu\nu}^i(q, p)$ can be calculated order by order in perturbation theory, provided the scale Q^2 is large enough for the strong coupling constant to be small. In the same manner, the contributing operator matrix elements with external partons may be evaluated. Finally, one can read off the Wilson coefficients from the partonic equivalent of Eq. 2.91.⁶ By identifying the nucleon OMEs (2.89) with the PDFs, one obtains the QCD improved parton model. At LO it coincides with the naive parton model, which we described in Sect. 2.2, as can be inferred from the discussion below Eq. 2.41. The improved parton model states that in the Bjorken limit at the level of twist $\tau = 2$ the unpolarized nucleon structure functions $F_i(x, Q^2)$ are obtained in Mellin space as products of the universal parton densities $f_i(N, \mu^2)$ with process–dependent Wilson coefficients $C_{i,(2,L)}(N, Q^2/\mu^2)$

$$F_{(2,L)}(N, Q^2) = \sum_i C_{i,(2,L)} \left(N, \frac{Q^2}{\mu^2} \right) f_i(N, \mu^2) \quad (2.94)$$

to all orders in perturbation theory. This property is also formulated in the factorization theorems [127, 129–134] cf. also [128] where it is essential that an inclusive, infrared–safe cross section is considered [153]. We have not yet dealt with the question of how renormalization is being performed. However, we have already intro-

⁶ Due to the optical theorem, one may also obtain the Wilson coefficients by calculating the inclusive hard scattering cross sections of a virtual photon with a quark(gluon) using the standard Feynman–rules and phase–space kinematics.

duced the scale μ^2 into the right-hand side of Eq. 2.94. This scale is called factorization scale. It describes a mass scale at which the separation of the structure functions into the perturbative hard scattering coefficients $C_{i,(2,L)}$ and the non-perturbative parton densities f_i can be performed. This choice is arbitrary at large enough scales and the physical structure functions do not depend on it. This independence is used in turn to establish the corresponding renormalization group equation [154–158] which describes the scale-evolution of the Wilson coefficients, parton densities and structure functions w.r.t. to μ^2 and Q^2 , cf. Refs. [89, 91, 152, 159–161] and Sect. 2.4

These evolution equations then predict scaling violations and are used to analyze experimental data in order to unfold the twist-2 parton distributions at some scale Q_0^2 , together with the QCD-scale Λ_{QCD} , cf. [159, 162, 163].

Before finishing this Section, we describe the quantities appearing in Eq. 2.94 in detail. Starting from the operators defined in Eqs. 2.86–2.88, three types of parton densities are expected. Since the question how heavy quarks are treated in this framework will be discussed in Chap. 3, we write the following equations for n_f light flavors in massless QCD. The gluon density is denoted by $G(n_f, N, \mu^2)$ and multiplies the gluonic Wilson coefficients $C_{g,(2,L)}(n_f, N, Q^2/\mu^2)$, which describe the interaction of a gluon with a photon and emerge for the first time at $O(\alpha_s)$. Each quark and its anti-quark have a parton density, denoted by $f_{k(\bar{k})}(n_f, N, \mu^2)$. These are grouped together into the flavor singlet combination $\Sigma(n_f, N, \mu^2)$ and a non-singlet combination $\Delta_k(n_f, N, \mu^2)$ as follows

$$\Sigma(n_f, N, \mu^2) = \sum_{l=1}^{n_f} \left[f_l(n_f, N, \mu^2) + f_{\bar{l}}(n_f, N, \mu^2) \right], \quad (2.95)$$

$$\Delta_k(n_f, N, \mu^2) = f_k(n_f, N, \mu^2) + f_{\bar{k}}(n_f, N, \mu^2) - \frac{1}{n_f} \Sigma(n_f, N, \mu^2). \quad (2.96)$$

The distributions multiply the quarkonic Wilson coefficients $C_{q,(2,L)}^{\text{S,NS}}(n_f, N, Q^2/\mu^2)$, which describe the hard scattering of a photon with a light quark. The complete factorization formula for the structure functions is then given by

$$F_{(2,L)}(n_f, N, Q^2) = \frac{1}{n_f} \sum_{k=1}^{n_f} e_k^2 \left[\Sigma(n_f, N, \mu^2) C_{q,(2,L)}^{\text{S}} \left(n_f, N, \frac{Q^2}{\mu^2} \right) + G(n_f, N, \mu^2) \right. \\ \left. \times C_{g,(2,L)}^{\text{S}} \left(n_f, N, \frac{Q^2}{\mu^2} \right) + n_f \Delta_k(n_f, N, \mu^2) C_{q,(2,L)}^{\text{NS}} \left(n_f, N, \frac{Q^2}{\mu^2} \right) \right]. \quad (2.97)$$

Note, that one usually splits the quarkonic S contributions into a NS and pure-singlet (PS) part via $\text{S} = \text{PS} + \text{NS}$. The perturbative expansions of the Wilson coefficients read

$$C_{g,(2,L)}^{\text{S}} \left(n_f, N, \frac{Q^2}{\mu^2} \right) = \sum_{i=1}^{\infty} a_s^i C_{g,(2,L)}^{(i),\text{S}} \left(n_f, N, \frac{Q^2}{\mu^2} \right), \quad (2.98)$$

$$C_{q,(2,L)}^{\text{PS}}\left(n_f, N, \frac{Q^2}{\mu^2}\right) = \sum_{i=2}^{\infty} a_s^i C_{q,(2,L)}^{(i),\text{PS}}\left(n_f, N, \frac{Q^2}{\mu^2}\right), \quad (2.99)$$

$$C_{q,(2,L)}^{\text{NS}}\left(n_f, N, \frac{Q^2}{\mu^2}\right) = \delta_2 + \sum_{i=1}^{\infty} a_s^i C_{q,(2,L)}^{(i),\text{NS}}\left(n_f, N, \frac{Q^2}{\mu^2}\right), \quad (2.100)$$

where $a_s \equiv \alpha_s/(4\pi)$ and

$$\delta_2 = 1 \text{ for } F_2 \text{ and } \delta_2 = 0 \text{ for } F_L. \quad (2.101)$$

These terms are at present known up to $O(a_s^3)$. The $O(a_s)$ terms have been calculated in Refs. [149, 164, 165] and the $O(a_s^2)$ contributions by various groups in Refs. [166–176]. The $O(a_s^3)$ terms have first been calculated for fixed moments in Refs. [177–180] and the complete result for all N has been obtained in Ref. [181].⁷

2.4 RGE–Improved Parton Model and Anomalous Dimensions

In the following, we present a derivation of the RGEs for the Wilson coefficients, and subsequently, the evolution equations for the parton densities. When calculating scattering cross sections in quantum field theories, they usually contain divergences of different origin. The infrared and collinear singularities are connected to the limit of soft—and collinear radiation, respectively. Due to the Bloch–Nordsieck theorem [183, 184] it is known that the infrared divergences cancel between virtual and bremsstrahlung contributions. The structure functions are inclusive quantities. Therefore, all final state collinear (mass) singularities cancel as well, which is formulated in the Lee–Kinoshita–Nauenberg theorem [185, 186]. Thus in case of the Wilson coefficients, only the initial state collinear divergences of the external light partons and the ultraviolet divergences remain. The latter are connected to the large scale behavior and are renormalized by a redefinition of the parameters of the theory, as the coupling constant, the masses, the fields, and the composite operators [187, 188]. This introduces a renormalization scale μ_r , which forms the subtraction point for renormalization. The scale which appears in the factorization formulas (2.94, 2.97) is denoted by μ_f and called factorization scale, cf. [127–133]. Its origin lies in the arbitrariness of the point at which short- and long-distance effects are separated and is connected to the redefinition of the bare parton densities by absorbing the initial state collinear singularities of the Wilson coefficients into them. Note, that one usually adopts dimensional regularization to regularize the infinities in perturbative calculations, cf. Chap. 4, which causes another scale μ to appear. It is associated to the mass dimension of the coupling constant in $D \neq 4$ dimensions. In principle all

⁷ Recently, the $O(a_s^3)$ Wilson coefficient for the structure function $x F_3(x, Q^2)$ was calculated in Ref. [182].

these three scales have to be treated separately, but we will set them equal in the subsequent analysis, $\mu = \mu_r = \mu_f$.

The renormalization group equations are obtained using the argument that all these scales are arbitrary and therefore physical quantities do not alter when changing these scales [154–157, 187, 188]. One therefore defines the total derivative w.r.t. to μ^2

$$\mathcal{D}(\mu^2) \equiv \mu^2 \frac{\partial}{\partial \mu^2} + \beta(a_s(\mu^2)) \frac{\partial}{\partial a_s(\mu^2)} - \gamma_m(a_s(\mu^2)) m(\mu^2) \frac{\partial}{\partial m(\mu^2)}. \quad (2.102)$$

Here the β -function and the anomalous dimension of the mass, γ_m , are given by

$$\beta(a_s(\mu^2)) \equiv \mu^2 \frac{\partial a_s(\mu^2)}{\partial \mu^2}, \quad (2.103)$$

$$\gamma_m(a_s(\mu^2)) \equiv -\frac{\mu^2}{m(\mu^2)} \frac{\partial m(\mu^2)}{\partial \mu^2}, \quad (2.104)$$

cf. Sects. 4.3 and 4.4. The derivatives have to be performed keeping the bare quantities \hat{a}_s , \hat{m} fixed. Additionally, we work in Feynman-gauge and therefore the gauge-parameter is not present in Eq. 2.102. In the following we will consider only one mass m . The composite operators (2.86–2.88) are renormalized introducing operator Z -factors

$$O_{q,r;\mu_1,\dots,\mu_N}^{\text{NS}} = Z^{\text{NS}}(\mu^2) \hat{O}_{q,r;\mu_1,\dots,\mu_N}^{\text{NS}}, \quad (2.105)$$

$$O_{i;\mu_1,\dots,\mu_N}^{\text{S}} = Z_{ij}^{\text{S}}(\mu^2) \hat{O}_{j;\mu_1,\dots,\mu_N}^{\text{S}}, \quad i = q, g, \quad (2.106)$$

where in the singlet case mixing occurs since these operators carry the same quantum numbers. The anomalous dimensions of the operators are defined by

$$\gamma_{qq}^{\text{NS}} = \mu Z^{-1,\text{NS}}(\mu^2) \frac{\partial}{\partial \mu} Z^{\text{NS}}(\mu^2), \quad (2.107)$$

$$\gamma_{ij}^{\text{S}} = \mu Z_{il}^{-1,\text{S}}(\mu^2) \frac{\partial}{\partial \mu} Z_{lj}^{\text{S}}(\mu^2). \quad (2.108)$$

We begin by considering the partonic structure functions calculated with external fields l . Here we would like to point out that we calculate matrix elements of currents, operators, etc. and not vacuum expectation values of time-ordered products with the external fields included. The anomalous dimensions of the latter therefore do not contribute [105] and they are parts of the anomalous dimensions of the composite operators, respectively. The RGE reads

$$\mathcal{D}(\mu^2) \mathcal{F}_{(2,L)}^l(N, Q^2) = 0. \quad (2.109)$$

On the partonic level, Eq. 2.93 takes the form

$$\mathcal{F}_{(2,L)}^l(N, Q^2) = \sum_j C_{j,(2,L)} \left(N, \frac{Q^2}{\mu^2} \right) \langle l | O_j(\mu^2) | l \rangle. \quad (2.110)$$

From the operator renormalization constants of the O_i , Eqs. 2.105, 2.106 the following RGE is derived for the matrix elements [152]

$$\sum_j \left(\mathcal{D}(\mu^2) \delta_{ij} + \frac{1}{2} \gamma_{ij}^{\text{S,NS}} \right) \langle l | O_j(\mu^2) | l \rangle = 0, \quad (2.111)$$

where we write the **S** and **NS** case in one equation for brevity and we remind the reader that in the latter case, $i, j, l = q$ only. Combining Eqs. 2.109–2.111 one can determine the RGE for the Wilson coefficients. It reads

$$\sum_i \left(\mathcal{D}(\mu^2) \delta_{ij} - \frac{1}{2} \gamma_{ij}^{\text{S,NS}} \right) C_{i,(2,L)} \left(N, \frac{Q^2}{\mu^2} \right) = 0. \quad (2.112)$$

The structure functions, which are observables, obey the same RGE as on the partonic level

$$\mathcal{D}(\mu^2) F_{(2,L)}(N, Q^2) = \mu^2 \frac{d}{d\mu^2} F_{(2,L)}(N, Q^2) = 0. \quad (2.113)$$

Using the factorization of the structure functions into Wilson coefficients and parton densities, Eqs. 2.94, 2.97 together with the RGE derived for the Wilson coefficients in Eq. 2.112, one obtains from the above formula the QCD evolution equations for the parton densities, cf. e.g. [89, 91, 152, 159–161]

$$\frac{d}{d \ln \mu^2} f_i^{\text{S,NS}}(n_f, N, \mu^2) = -\frac{1}{2} \sum_j \gamma_{ij}^{\text{S,NS}} f_j^{\text{S,NS}}(n_f, N, \mu^2). \quad (2.114)$$

Eq. 2.114 describes the change of the parton densities w.r.t. the scale μ . In the more familiar matrix notation, these equations read

$$\frac{d}{d \ln \mu^2} \begin{pmatrix} \Sigma(n_f, N, \mu^2) \\ G(n_f, N, \mu^2) \end{pmatrix} = -\frac{1}{2} \begin{pmatrix} \gamma_{qq} & \gamma_{qg} \\ \gamma_{gq} & \gamma_{gg} \end{pmatrix} \begin{pmatrix} \Sigma(n_f, N, \mu^2) \\ G(n_f, N, \mu^2) \end{pmatrix}, \quad (2.115)$$

$$\frac{d}{d \ln \mu^2} \Delta_k(n_f, N, \mu^2) = -\frac{1}{2} \gamma_{qq}^{\text{NS}} \Delta_k(n_f, N, \mu^2), \quad (2.116)$$

where we have used the definition for the parton densities in Eqs. 2.95, 2.96. The anomalous dimensions in the above equations can be calculated order by order in perturbation theory. At LO [68–70] and NLO [189–195] they have been known for a

long time. The NNLO anomalous dimension were calculated first for fixed moments in Refs. [178–180] and the complete result for all moments has been obtained in Refs. [196, 197].⁸ As described, the PDFs are non-perturbative quantities and have to be extracted at a certain scale from experimental data using the factorization relation (2.94). If the scale μ^2 is large enough to apply perturbation theory, the evolution equations can be used to calculate the PDFs at another perturbative scale, which provides a detailed QCD test comparing to precision data. There are similar evolution equations for the structure functions and Wilson coefficients, cf. e.g. [89, 91, 152, 159–161]. Different groups analyze the evolution of the parton distribution functions based on precision data from deep-inelastic scattering experiments and other hard scattering cross sections. Analyses were performed by the Dortmund group [198–206] by Alekhin et. al. [207, 208] Blümlein et. al. [209, 210] the MSTW—[211] QTEQ—[212] and the NNPDF—collaborations [213]. The PDFs determined in this way can e.g. be used as input data for the pp collisions at the LHC, since they are universal quantities and only relate to the structure of the proton and not to the particular kind of scattering events considered. Apart from performing precision analyses of the PDFs, one can also use the evolution equations to determine a_s more precisely [198, 199, 205–211].

The evolution Eqs. 2.114–2.116 are written for moments only. The representation in x -space is obtained by using (2.65–2.67) and is usually expressed in terms of the splitting functions $P_{ij}(x)$, [94]. At the level of twist-2 the latter are connected to the anomalous dimensions by the Mellin-transform

$$\gamma_{ij}(N) = -\mathbf{M}[P_{ij}](N) . \quad (2.117)$$

The behavior of parton distribution functions in the small x region attracted special interest due to possibly new dynamical contributions, such as Glauber-model based screening corrections [214–220] and the so-called BFKL contributions, a ‘leading singularity’ resummation in the anomalous dimensions for all orders in the strong coupling constant [221–225]. For both effects there is no evidence yet in the data both for $F_2(x, Q^2)$ and $F_L(x, Q^2)$, beyond the known perturbative contributions to $O(a_s^3)$. This does not exclude that at even smaller values of x contributions of this kind will be found. The BFKL contributions were investigated on the basis of a consistent renormalization group treatment, together with the fixed order contributions in Refs. [226–230]. One main characteristic, comparing with the fixed order case, is that several sub-leading series, which are unknown, are required to stabilize the results, see also [231]. This aspect also has to be studied within the framework of recent approaches [232, 233].

⁸ Note that from our convention in Eqs. 2.107, 2.108 follows a relative factor 2 between the anomalous dimensions considered in this work compared to Refs. [196, 197].

References

1. L.W. Mo, C. Peck, 8-GeV/c *Spectrometer*, SLAC-TN-65-029 (1965)
2. R.E. Taylor, Nucleon form-factors above 6-GeV, in *Proceedings of the International Symposium on Electron and Photon Interactions at High Energies*, SLAC, September 5–9, 1967, (SLAC, Stanford CA, 1967), SLAC-PUB-0372, pp. 78
3. D.H. Coward et al., Phys. Rev. Lett. **20**, 292 (1968)
4. W.K.H. Panofsky, Low q^2 electrodynamics, elastic and inelastic electron (and muon) scattering, *Proceedings of 14th International Conference on High-Energy Physics*, Vienna, 1968, J. Prentki and J. Steinberger, eds., (CERN, Geneva, 1968), pp. 23
5. E.D. Bloom et al., Phys. Rev. Lett. **23**, 930 (1969)
6. M. Breidenbach et al., Phys. Rev. Lett. **23**, 935 (1969)
7. H.W. Kendall, Rev. Mod. Phys. **63**, 597 (1991)
8. R.E. Taylor, Rev. Mod. Phys. **63**, 573 (1991)
9. J.I. Friedman, Rev. Mod. Phys. **63**, 615 (1991)
10. W. Albrecht et al., Phys. Lett. **B28**, 225 (1968)
11. W. Albrecht et al., Nucl. Phys. **B13**, 1 (1969)
12. W. Albrecht, et al., Separation of sigma-L and sigma-t in the region of deep inelastic electron - proton scattering, DESY-69-046 (1969)
13. J.D. Bjorken, Phys. Rev. **179**, 1547 (1969)
14. R.P. Feynman, The behavior of hadron collisions at extreme energies, in *Proceedings of 3rd International Conference on High Energy Collisions*, Stony Brook, 1969, C.N. Yang, J.A. Cole, M. Good, R. Hwa, and J. Lee-Franzini, eds., (Gordon and Breach, New York, 1970), pp. 237
15. R.P. Feynman, Phys. Rev. Lett. **23**, 1415 (1969)
16. J.D. Bjorken, E.A. Paschos, Phys. Rev. **185**, 1975 (1969)
17. M. Gell-Mann, Phys. Lett. **8**, 214 (1964)
18. G. Zweig, An $SU(3)$ model for the strong interaction symmetry and its breaking, CERN-TH-401, 412 (1964)
19. J.S. Bell, R. Jackiw, Nuovo Cim. **A60**, 47 (1969)
20. S.L. Adler, Phys. Rev. **177**, 2426 (1969)
21. R.A. Bertlmann, *Anomalies in quantum field theory*, (Clarendon, Oxford, 1996) pp. 566.
22. S. Stein et al., Phys. Rev. **D12**, 1884 (1975)
23. W.B. Atwood et al., Phys. Lett. **B64**, 479 (1976)
24. A. Bodek et al., Phys. Rev. **D20**, 1471 (1979)
25. M.D. Mestayer et al., Phys. Rev. **D27**, 285 (1983)
26. EMC collaboration, O. Allkofer, et al., Nucl. Instr. Meth. **179**, 445 (1981)
27. EMC collaboration, J. J. Aubert et al., Nucl. Phys. **B259**, 189 (1985)
28. D. Bollini et al., Nucl. Instr. Meth. **204**, 333 (1983)
29. BCDMS collaboration, A.C. Benvenuti, et al., Nucl. Instr. Meth. **A226**, 330 (1984)
30. BCDMS collaboration, A.C. Benvenuti, et al., Phys. Lett. **B195**, 91 (1987)
31. BCDMS collaboration, A.C. Benvenuti, et al., Phys. Lett. **B223**, 485 (1989)
32. BCDMS collaboration, A.C. Benvenuti, et al., Phys. Lett. **B237**, 592 (1990)
33. NMC collaboration, P. Amaudruz, et al., Nucl. Phys. **B371**, 3 (1992)
34. NMC collaboration, P. Amaudruz, et al., Phys. Lett. **B295**, 159 (1992)
35. NMC collaboration, M. Arneodo, et al., Phys. Lett. **B364**, 107 (1995), hep-ph/9509406
36. R. Clifft, N. Doble, Proposed Design of a High-Energy, High Intensity Muon Beam for the SPS North Experimental Area, CERN/LAB. II/EA/74-2 (1974)
37. C. Chang et al., Phys. Rev. Lett. **35**, 901 (1975)
38. Y. Watanabe et al., Phys. Rev. Lett. **35**, 898 (1975)
39. D.J. Fox et al., Phys. Rev. Lett. **33**, 1504 (1974)
40. H.L. Anderson et al., Phys. Rev. **D20**, 2645 (1979)
41. E665 collaboration, M.R. Adams, et al., Nucl. Instrum. Meth **A291**, 533 (1990)

42. E665 collaboration, M.R. Adams, et al., Phys. Rev. **D54**, 3006 (1996)
43. T. Sloan, R. Voss, G. Smadja, Phys. Rept. **162**, 45 (1988)
44. CHARM collaboration, M. Jonker, et al., Phys. Lett. **B109**, 133 (1982)
45. CHARM collaboration, F. Bergsma, et al., Phys. Lett. **B123**, 269 (1983)
46. CHARM collaboration, F. Bergsma, et al., Phys. Lett. **B153**, 111 (1985)
47. J.P. Berge et al., Z. Phys. **D49**, 187 (1991)
48. M. Holder et al., Nucl. Instrum. Meth. **151**, 69 (1978)
49. CDHSW collaboration, W. Von Ruden, IEEE Trans. Nucl. Sci. **29**, 360 (1982)
50. Birmingham-CERN-Imperial College-München(MPI)-Oxford collaboration, G. T. Jones, et al., Z. Phys. **C62**, 575 (1994)
51. G. Harigel, *BEBC user's handbook*. (CERN, Geneva, 1977)
52. CCFR collaboration, M.H. Shaevitz, et al., Nucl. Phys. Proc. Suppl. **38**, 188 (1995)
53. W.K. Sakumoto et al., Nucl. Instrum. Meth. **A294**, 179 (1990)
54. B.J. King et al., Nucl. Instrum. Meth. A **302**, 254 (1991)
55. Aachen-Bonn-CERN-London-Oxford-Saclay collaboration, P.C. Bosetti, et al., Nucl. Phys. **B142**, 1 (1978)
56. de J.G.H. Groot et al., Z. Phys. C **1**, 143 (1979)
57. S.M. Heagy et al., Phys. Rev. D **23**, 1045 (1981)
58. Gargamelle SPS collaboration, J.G. Morfin, et al., Phys. Lett. **B104**, 235 (1981)
59. Aachen-Bonn-CERN-Democritos-London-Oxford-Saclay collaboration, P.C. Bosetti, et al., Nucl. Phys. **B203**, 362 (1982)
60. H. Abramowicz et al., Z. Phys. C **17**, 283 (1983)
61. D. MacFarlane et al., Z. Phys. C **26**, 1 (1984)
62. D. Allasia et al., Z. Phys. C **28**, 321 (1985)
63. M. Diemoz, F. Ferroni, E. Longo, Phys. Rept. **130**, 293 (1986)
64. F. Eisele, Rept. Prog. Phys. **49**, 233 (1986)
65. S.R. Mishra, F. Sciulli, Ann. Rev. Nucl. Part. Sci. **39**, 259 (1989)
66. Winter K., ed., *Neutrino physics*, Camb. Monogr. Part. Phys. Nucl. Phys. Cosmol. Vol. **1**, (Cambridge University Press, Cambridge, 1991), 670 p
67. N. Schmitz, *Neutrino physics*, (Teubner, Stuttgart, 1997) pp. 478.
68. D.J. Gross, F. Wilczek, Phys. Rev. D **8**, 3633 (1973)
69. D.J. Gross, F. Wilczek, Phys. Rev. **D9**, 980 (1974)
70. H. Georgi, H.D. Politzer, Phys. Rev. **D9**, 416 (1974)
71. HERA - a proposal for a large electron proton colliding beam facility at DESY, (Hamburg, DESY, 1981), DESY HERA 81-10, 292 p
72. R.D. Peccei, ed., *Proceedings, HERA Workshop*, Hamburg, F.R. Germany, October 12-14, 1987. Vol. **1,2**, 937 p
73. W. Buchmüller, G. Ingelman, eds., *Proceedings, Physics at HERA Workshop*, Hamburg, F.R. Germany, October 29-30, 1991. Vol. **1-3**, 1566 p
74. J. Blümlein, T. Riemann, eds., *Deep inelastic scattering. Proceedings, Zeuthen Workshop on Elementary Particle Theory, Teupitz, Germany, April 6-10, 1992*, Nucl. Phys. Proc. Suppl. **B29A**, 295 p. (1992)
75. HERA - The new frontier for QCD. *Proceedings, Workshop*, Durham, UK, March 21-26, 1993, J. Phys. **G19** (1993), pp. 1427
76. J.F. Mathiot, J. Tran Thanh Van, eds., *Prepared for 6th Rencontres de Blois: The Heart of the Matter: from Nuclear Interactions to Quark - Gluon Dynamics*, Blois, France, 20-25 Jun 1994, (Ed. Frontieres, Gif-sur-Yvette, 1995), 556 p
77. J. Blümlein, W.D. Nowak, eds., *Prospects of spin physics at HERA. Proc., Workshop*, Zeuthen, Germany, August 28-31, 1995, DESY-95-200, (DESY, Hamburg, 1995), 387 p
78. G. Ingelman, A. De Roeck, R. Klanner, eds., *Future physics at HERA. Proceedings, Workshop*, Hamburg, Germany, September 25, 1995-May 31, 1996. Vol. **1,2**, DESY-96-235, 1231 p

79. J. Blümlein, A. De Roeck, T. Gehrmann, W. D. Nowak, eds., *Deep inelastic scattering off polarized targets: Theory meets experiment. Physics with polarized protons at HERA. Proceedings, Workshops, SPIN'97, Zeuthen, Germany, September 1–5, 1997 and Hamburg, Germany, March–September 1997*, DESY-97-200
80. J. Blümlein, W.D. Nowak, G. Schnell, eds., *Transverse spin physics*, Proceedings, Topical Workshop, Zeuthen, Germany, July 9–11, 2001, DESY-Zeuthen-01-01, Aug 2001. 374 p
81. H1 collaboration, I. Abt, et al., *The H1 detector at HERA*, DESY-93-103 (1993), 194 p
82. ZEUS collaboration, M. Derrick, et al., *Phys. Lett.* **B303**, 183 (1993)
83. HERMES collaboration, K. Ackerstaff, et al., *Nucl. Instrum. Meth.* **A417**, 230 (1998), hep-ex/9806008
84. E. Hartouni et al., *HERA-B: An experiment to study CP violation in the B system using an internal target at the HERA proton ring*. Design report, DESY-PRC-95-01 (1995), 491 p
85. K.G. Wilson, *Phys. Rev.* **179**, 1499 (1969)
86. W. Zimmermann, *Lect. on Elementary Particle Physics and Quantum Field Theory*, Brandeis Summer Inst., Vol. **1**, (MIT Press, Cambridge, 1970), pp. 395.
87. Y. Frishman, *Annals Phys.* **66**, 373 (1971)
88. R.A. Brandt, G. Preparata, *Nucl. Phys.* **B27**, 541 (1972)
89. E. Reya, *Phys. Rept.* **69**, 195 (1981)
90. T. Muta, *Foundations of Quantum Chromodynamics*, World Sci. Lect. Notes Phys. 57, (World Scientific, Singapore, 1998), 2nd edition
91. R.G. Roberts, *The Structure of the proton: Deep inelastic scattering*, (Cambridge University Press, Cambridge, 1990) pp. 182.
92. J.B. Kogut, L. Susskind, *Phys. Rept.* **8**, 75 (1973)
93. T.-M. Yan, *Ann. Rev. Nucl. Part. Sci.* **26**, 199 (1976)
94. G. Altarelli, G. Parisi, *Nucl. Phys.* **B126**, 298 (1977)
95. J. Blümlein, M. Klein, *Nucl. Instrum. Meth.* **A329**, 112 (1993)
96. J. Blümlein, *Z. Phys.* **C65**, 293 (1995), hep-ph/9403342
97. A. Arbuzov, D.Y. Bardin, J. Blümlein, L. Kalinovskaya, T. Riemann, *Comput. Phys. Commun.* **94**, 128 (1996), hep-ph/9511434 and references therein
98. J.D. Bjorken, *Phys. Rev.* **D1**, 1376 (1970)
99. J. Blümlein, M. Klein, T. Naumann, T. Riemann, *Structure functions, quark distributions and Λ_{QCD} at HERA in *Proceedings of DESY Theory Workshop on Physics at HERA* (ed. R.D. Peccei), Hamburg, F.R. Germany, 12–14 October 1987, Vol **1**, 67 pp*
100. A. Kwiatkowski, H. Spiesberger, H.J. Möhring, *Comp. Phys. Commun.* **69**, 155 (1992), and references therein
101. J. Engelen, P. Kooijman, *Prog. Part. Nucl. Phys.* **41**, 1 (1998)
102. H. Abramowicz, A. Caldwell, *Rev. Mod. Phys.* **71**, 1275 (1999), hep-ex/9903037
103. H1 collaboration, F.D. Aaron et al., *Phys. Lett.* **B665**, 139 (2008), hep-ex/0805.2809
104. J. Blümlein, B. Geyer, D. Robaschik, *Nucl. Phys.* **B560**, 283 (1999), hep-ph/9903520
105. F.J. Yndurain, *The theory of quark and gluon interactions*, 4th edn. (Springer, Berlin, 2006) pp. 474.
106. R. Field, *Applications of perturbative QCD*, (Addison-Wesley, Redwood City, 1989) pp. 366.
107. LHPC collaboration, D. Dolgov, et al., *Phys. Rev.* **D66**, 034506 (2002), hep-lat/0201021
108. QCDSF collaboration, M. Göckeler, et al., *PoS LAT 2007*, 147 (2007), hep-lat/0710.2489
109. ETM collaboration, R. Baron, et al., *PoS LAT 2007*, 153 (2007), hep-lat/0710.1580
110. W. Bietenholz, et al., *PoS LAT 2008*, 149 (2008), hep-lat/0808.3637
111. S.N. Syritsyn, et al., *PoS LAT 2008*, 169 (2008), hep-lat/0903.3063
112. C. Itzykson, J. Zuber, *Quantum Field Theory*, (McGraw-Hill, New York, 1980) pp. 705.
113. J. Blümlein, N. Kochelev, *Nucl. Phys.* **B498**, 285 (1997), hep-ph/9612318
114. J. Blümlein, A. Tkabladze, *Nucl. Phys.* **B553**, 427 (1999), hep-ph/9812478
115. E. Rutherford, *Phil. Mag.* **21**, 669 (1911)
116. R.W. Mcallister, R. Hofstadter, *Phys. Rev.* **102**, 851 (1956)

117. D.N. Olson, H.F. Schopper, R.R. Wilson, Phys. Rev. Lett. **6**, 286 (1961)
118. R. Hofstadter, *Electron scattering and nuclear and nucleon structure. A collection of reprints with an introduction*, (New York, Benjamin, 1963), 690 p
119. R.P. Feynman, *Photon-hadron interactions*, (Benjamin Press, Reading, 1972) pp. 282.
120. C. Nash, Nucl. Phys. **B31**, 419 (1971)
121. P.V. Landshoff, J.C. Polkinghorne, Phys. Rept. **5**, 1 (1972)
122. J.D. Jackson, G.G. Ross, R.G. Roberts, Phys. Lett. **B226**, 159 (1989)
123. R.G. Roberts, G.G. Ross, Phys. Lett. **B373**, 235 (1996), hep-ph/9601235
124. J. Blümlein, N. Kochelev, Phys. Lett. **B381**, 296 (1996), hep-ph/9603397
125. J. Blümlein, V. Ravindran, and W.L. van Neerven, Phys. Rev. **D68**, 114004 (2003), hep-ph/0304292
126. F.E. Close, *An Introduction to Quarks and Partons*, (Academic Press, London, 1979) pp. 481.
127. S.B. Libby, G. Sterman, Phys. Rev. **D18**, 4737 (1978)
128. J.C. Collins, D.E. Soper, Ann. Rev. Nucl. Part. Sci. **37**, 383 (1987)
129. D. Amati, R. Petronzio, G. Veneziano, Nucl. Phys. **B140**, 54 (1978)
130. S.B. Libby, G. Sterman, Phys. Rev. **D18**, 3252 (1978)
131. A.H. Mueller, Phys. Rev. **D18**, 3705 (1978)
132. J.C. Collins, G. Sterman, Nucl. Phys. **B185**, 172 (1981)
133. G.T. Bodwin, Phys. Rev. **D31**, 2616 (1985); [Erratum-ibid.] **D34**, 3932 (1986)
134. J.C. Collins, D.E. Soper, G. Sterman, Nucl. Phys. **B261**, 104 (1985)
135. P. Mulders, *Quantum Chromodynamics and Hard Scattering Processes*, Lectures, Dutch Research School for Theoretical Physics, Dalfsen, January 1996, and Dutch Research School for Subatomic Physics, Beekbergen, February, 1996, (NIKHEF, Amsterdam, The Netherlands)
136. C.G. Callan, D.J. Gross, Phys. Rev. Lett. **22**, 156 (1969)
137. S.D. Drell, T.-M. Yan, Ann. Phys. **66**, 578 (1971)
138. J. Blümlein, *Introduction into QCD*, Lecture Notes (1997)
139. R. Jackiw, *Canonical light-cone commutators and their applications in* (49), pp 1
140. R.L. Jaffe, *Deep Inelastic Scattering with Application to nuclear targets*, Lectures presented at the Los Alamos School on Quark Nuclear Physics, Los Alamos, NM, 10–14 June 1985, M.B. Johnson and A. Picklesimer, eds., (Wiley, New York, 1986), pp. 82
141. Y. Frishman, Phys. Rept. **13**, 1 (1974)
142. B. Geyer, D. Robaschik, E. Wieczorek, Fortschr. Phys. **27**, 75 (1979)
143. A.H. Mueller, Phys. Rept. **73**, 237 (1981)
144. J. Blümlein, Comput. Phys. Commun. **133**, 76 (2000), hep-ph/0003100
145. J. Blümlein, S.-O. Moch, Phys. Lett. **B614**, 53 (2005), hep-ph/0503188
146. E. Carlson, *Sur une classe de séries de Taylor*, PhD Thesis, Uppsala, 1914
147. E. Titchmarsh, *Theory of Functions*. (Oxford University Press, Oxford, 1939) Chapt. 9.5
148. D.J. Gross, S.B. Treiman, Phys. Rev. **D4**, 1059 (1971)
149. W.A. Bardeen, A.J. Buras, D.W. Duke, T. Muta, Phys. Rev. **D18**, 3998 (1978)
150. L.D. Landau, Nucl. Phys. **13**, 181 (1959)
151. J.D. Bjorken, *Experimental tests of quantum electrodynamics and spectral representations of Green's functions in perturbation theory*, PhD Thesis, RX-1037 (1959)
152. A.J. Buras, Rev. Mod. Phys. **52**, 199 (1980)
153. A. Bassetto, M. Ciafaloni, G. Marchesini, Phys. Rept. **100**, 201 (1983)
154. E.C.G. Stückelberg, A. Petermann, Helv. Phys. Acta **24**, 317 (1951)
155. M. Gell-Mann, F.E. Low, Phys. Rev. **95**, 1300 (1954)
156. N.N. Bogolyubov, D.V. Shirkov, *Introduction to the theory of quantized fields*, (Interscience, New York, 1959) pp. 720.
157. K. Symanzik, Commun. Math. Phys. **18**, 227 (1970)
158. C.G. Callan, Phys. Rev. **D2**, 1541 (1970)
159. G. Altarelli, Ann. Rev. Nucl. Part. Sci. **39**, 357 (1989)
160. J.F. Owens, W.-K. Tung, Ann. Rev. Nucl. Part. Sci. **42**, 291 (1992)

161. J. Blümlein, On the Theoretical Status of Deep Inelastic Scattering, (1995), hep-ph/9512272
162. D.W. Duke, R.G. Roberts, Phys. Rept. **120**, 275 (1985)
163. S. Bethke, J.E. Pilcher, Ann. Rev. Nucl. Part. Sci. **42**, 251 (1992)
164. A. Zee, F. Wilczek, S.B. Treiman, Phys. Rev. **D10**, 2881 (1974)
165. W. Furmanski, R. Petronzio, Z. Phys. **C11**, 293 (1982), and references therein
166. D.W. Duke, J.D. Kimel, G.A. Sowell, Phys. Rev. **D25**, 71 (1982)
167. A. Devoto, D.W. Duke, J.D. Kimel, G.A. Sowell, Phys. Rev. **D30**, 541 (1984)
168. D.I. Kazakov, A.V. Kotikov, Nucl. Phys. **B307**, 721 (1988)
169. D.I. Kazakov, A.V. Kotikov, G. Parente, O.A. Sampayo, J. Sanchez Guillen, Phys. Rev. Lett. **65**, 1535 (1990)
170. J. Sanchez Guillen, J. Miramontes, M. Miramontes, G. Parente, O.A. Sampayo, Nucl. Phys. **B353**, 337 (1991)
171. van W.L. Neerven, E.B. Zijlstra, Phys. Lett. **B272**, 127 (1991)
172. van W.L. Neerven, E.B. Zijlstra, Phys. Lett. **B273**, 476 (1991)
173. van W.L. Neerven, E.B. Zijlstra, Nucl. Phys. **B383**, 525 (1992)
174. D.I. Kazakov, A.V. Kotikov, Phys. Lett. **B291**, 171 (1992)
175. S.A. Larin, J.A.M. Vermaseren, Z. Phys. **C57**, 93 (1993)
176. S. Moch, J.A.M. Vermaseren, Nucl. Phys. **B573**, 853 (2000), hep-ph/9912355
177. S.A. Larin, van T. Ritbergen, J.A.M. Vermaseren, Nucl. Phys. **B427**, 41 (1994)
178. S.A. Larin, P. Nogueira, T. van Ritbergen, J.A.M. Vermaseren, Nucl. Phys. **B492**, 338 (1997), hep-ph/9605317
179. A. Retey, J.A.M. Vermaseren, Nucl. Phys. **B604**, 281 (2001), hep-ph/0007294
180. J. Blümlein, J.A.M. Vermaseren, Phys. Lett. **B606**, 130 (2005), hep-ph/0411111
181. J.A.M. Vermaseren, A. Vogt, S. Moch, Nucl. Phys. **B724**, 3 (2005), hep-ph/0504242
182. S. Moch, J.A.M. Vermaseren, A. Vogt, Nucl. Phys. **B813**, 220 (2009), hep-ph/0812.4168
183. F. Bloch, A. Nordsieck, Phys. Rev. **52**, 54 (1937)
184. D.R. Yennie, S.C. Frautschi, H. Suura, Ann. Phys. **13**, 379 (1961)
185. T. Kinoshita, J. Math. Phys. **3**, 650 (1962)
186. T.D. Lee, M. Nauenberg, Phys. Rev. **133**, B1549 (1964)
187. A. Peterman, Phys. Rept. **53**, 157 (1979)
188. J.C. Collins, *Renormalization*, (Cambridge University Press, Cambridge, 1984) pp. 380.
189. E.G. Floratos, D.A. Ross, C.T. Sachrajda, Nucl. Phys. **B129**, 66 (1977); [Erratum-ibid.] **B139**, 545 (1978)
190. E.G. Floratos, D.A. Ross, C.T. Sachrajda, Nucl. Phys. **B152**, 493 (1979)
191. A. Gonzalez-Arroyo, C. Lopez, F.J. Yndurain, Nucl. Phys. **B153**, 161 (1979)
192. A. Gonzalez-Arroyo, C. Lopez, Nucl. Phys. **B166**, 429 (1980)
193. G. Curci, W. Furmanski, R. Petronzio, Nucl. Phys. **B175**, 27 (1980)
194. W. Furmanski, R. Petronzio, Phys. Lett. **B97**, 437 (1980)
195. R. Hamberg, van W.L. Neerven, Nucl. Phys. **B379**, 143 (1992)
196. S. Moch, J.A.M. Vermaseren, A. Vogt, Nucl. Phys. **B688**, 101 (2004), hep-ph/0403192
197. A. Vogt, S. Moch, J.A.M. Vermaseren, Nucl. Phys. **B691**, 129 (2004), hep-ph/0404111
198. M. Glück, E. Reya, C. Schuck, Nucl. Phys. **B754**, 178 (2006), hep-ph/0604116
199. M. Glück, E. Hoffmann, E. Reya, Z. Phys. **C13**, 119 (1982)
200. M. Glück, R.M. Godbole, E. Reya, Z. Phys. **C41**, 667 (1989)
201. M. Glück, E. Reya, A. Vogt, Z. Phys. **C48**, 471 (1990)
202. M. Glück, E. Reya, A. Vogt, Z. Phys. **C53**, 127 (1992)
203. M. Glück, E. Reya, A. Vogt, Z. Phys. **C67**, 433 (1995)
204. M. Glück, E. Reya, A. Vogt, Eur. Phys. J. **C5**, 461 (1998), hep-ph/9806404
205. M. Glück, P. Jimenez-Delgado, E. Reya, Eur. Phys. J. **C53**, 355 (2008), hep-ph/0709.0614
206. P. Jimenez-Delgado, E. Reya, Phys. Rev. **D79**, 074023 (2009), hep-ph/0810.4274
207. S. Alekhin, K. Melnikov, F. Petriello, Phys. Rev. **D74**, 054033 (2006), hep-ph/0606237
208. S. Alekhin, JETP Lett. **82**, 628 (2005), hep-ph/0508248

209. J. Blümlein, H. Böttcher, A. Guffanti, Nucl. Phys. Proc. Suppl. **135**, 152 (2004), hep-ph/0407089
210. J. Blümlein, H. Böttcher, A. Guffanti, Nucl. Phys. **B774**, 182 (2007), hep-ph/0607200
211. A.D. Martin, W.J. Stirling, R.S. Thorne, G. Watt, Eur. Phys. J. **C63**, 189 (2009), hep-ph/0901.0002
212. CTEQ collaboration, H.L. Lai et al., Eur. Phys. J. **C12**, 375 (2000), hep-ph/9903282
213. NNPDF collaboration, R.D. Ball et al., Nucl. Phys. **B809**, 1(2009), hep-ph/0808.1231
214. L.V. Gribov, E.M. Levin, M.G. Ryskin, Nucl. Phys. **B188**, 555 (1981)
215. A.H. Mueller, J.-W. Qiu, Nucl. Phys. **B268**, 427 (1986)
216. J.C. Collins, J. Kwiecinski, Nucl. Phys. **B335**, 89 (1990)
217. J. Bartels, G.A. Schuler, J. Blümlein, Z. Phys. **C50**, 91 (1991)
218. M. Altmann, M. Glück, E. Reya, Phys. Lett. **B285**, 359 (1992)
219. V. Del Duca, An introduction to the perturbative QCD pomeron and to jet physics at large rapidities, (1995), hep-ph/9503226
220. L.N. Lipatov, Phys. Rept. **286**, 131 (1997), hep-ph/9610276
221. V.S. Fadin, E.A. Kuraev, L.N. Lipatov, Phys. Lett. **B60**, 50 (1975)
222. I.I. Balitsky, L.N. Lipatov, Sov. J. Nucl. Phys. **28**, 822 (1978)
223. R. Kirschner, L.N. Lipatov, Nucl. Phys. **B213**, 122 (1983)
224. J. Bartels, B.I. Ermolaev, M.G. Ryskin, Z. Phys. **C72**, 627 (1996), hep-ph/9603204
225. V.S. Fadin, L.N. Lipatov, Phys. Lett. **B429**, 127 (1998), hep-ph/9802290
226. J. Blümlein, A. Vogt, Phys. Lett. **B370**, 149 (1996), hep-ph/9510410
227. J. Blümlein, A. Vogt, Acta Phys. Polon. **B27**, 1309 (1996), hep-ph/9603450
228. J. Blümlein, A. Vogt, Phys. Lett. **B386**, 350 (1996), hep-ph/9606254
229. J. Blümlein, A. Vogt, Phys. Rev. **D58**, 014020 (1998), hep-ph/9712546
230. J. Blümlein, V. Ravindran, W.L. van Neerven, A. Vogt, (1998), hep-ph/9806368
231. J. Blümlein, W.L. van Neerven, Phys. Lett. **B450**, 412 (1999), hep-ph/9811519
232. G. Altarelli, R.D. Ball, S. Forte, Nucl. Phys. **B799**, 199 (2008), hep-ph/0802.0032
233. M. Ciafaloni, D. Colferai, G.P. Salam, A.M. Stasto, JHEP **08**, 046 (2007), hep-ph/0707.1453

Charm Production in Deep Inelastic Scattering
Mellin Moments of Heavy Flavor Contributions to
 $F_2(x, Q^2)$ at NNLO

Klein, S.

2012, XIV, 242 p., Hardcover

ISBN: 978-3-642-23285-5